

AFM examination of sol–gel matrices doped with photosensitizers

KATARZYNA WYSOCKA¹, AGNIESZKA ULATOWSKA-JARŻA¹, JOANNA BAUER¹,
IWONA HOŁOWACZ¹, BOGDAN SAVU², GEORGE STANCIU², HALINA PODBIELSKA¹

¹Bio-Optics Group, Institute of Biomedical Engineering and Instrumentation and Institute of Physics,
Wrocław University of Technology, Wybrzeże Wyspiańskiego 27, Poland

²Center for Microscopy – Microanalysis and Information Processing,
University “Politehnica” of Bucharest, 313 Splaiul Independentei 060042 Bucharest, Romania

Various compounds may be entrapped into the sol–gel materials, including the photosensitive agents. The nanostructure of the final material depends on the matrix itself, as well as on the structural properties of doped compound. In this work, sol–gel matrices were produced from silica based precursor tetraethoxysilan (TEOS) in the form of single layers deposited on microscopic glasses. Materials were produced with molar ratios $R = 20, 32, 40$ (R – the number of solvent (ethanol) moles to the number of precursor (TEOS) moles). Additionally, for each material two various concentrations of photosensitizers were prepared (0.5 mg/ml and 0.05 mg/ml). On the basis of AFM images from Atomic Force Microscope Quesant 350, the following roughness parameters were evaluated: roughness average, peak–peak height, surface skewness and fractal dimension. The roughness average S_a parameter gives information about the statistical average properties. The peak–peak height S_y is defined as the height difference between the highest and the lowest pixel in the image. The surface skewness S_{sk} describes the asymmetry of the height distribution histogram. The fractal dimension S_{fd} is calculated for the different angles by analyzing the Fourier amplitude spectrum. Comparing the results we stated that average roughness increases with increasing R factor for protoporphyrine IX dimethylester (PPIX) (dimethyl-8,13-divinyl-3,7,12,17-tetramethyl-21H,23H-porphine-2,18-dipropionate) and photolon (18-carboxy-20-(carboxymethyl)-8-ethenyl-13-ethyl-2,3-dihydro-3,7,12,17-tetramethyl-21H,23H-porphin-2-propionic acid) in higher concentrations. This means that photosensitizers used as dopants influence the smoothness of sol–gel matrix. We also noticed that the smallest roughness is observed in the material doped with PPIX in higher concentration. This was stated for all the images analyzed. This indicates that sol–gel matrix enclosures the PPIX molecules, resulting in smooth material.

Keywords: atomic force microscope (AFM), sol–gel material nanostructure, photosensitizers.

1. Introduction

A combination of inorganic and organic networks by exploiting sol–gel technology, enables us to synthesize hybrid organic–inorganic matrices, thus to design new materials with useful properties for a wide range of applications. In this way, glasses, ceramics and thin films or fibers, may be produced directly from solution.

The range of recent applications of sol–gel derived materials is really very wide and includes biomedical, environmental, photovoltaic and many other applications [1–4]. Silica based sol–gel materials can also be used for construction of various optoelectronic devices, including optodes of optical sensors [5–7].

Absorption and fluorescence characteristics of many compounds, *e.g.*, tetrapyrrolic macrocycles, are sensitive to changes in their (molecular) environment, for instance, porphyrines may be immobilized in sol–gel matrices and serve as sensing agents [8, 9]. Recently, we have demonstrated that both agents: chlorin derivative photolon, as well as protoporphyrine immobilized in sol–gel matrices react to changes of pH in environment, thus may be used for sensing purposes [10, 11]. We examined the performance of pH sensors, constructed as a doped sol–gel coating deposited on optical fiber core. We observed that performance of the sensor depends on the kind of dopant used (photosensitizer), its concentration, as well as factor R (solvent to precursor molar ratio).

The performance of such devices is also connected with thermal and chemical stability, transparency, as well as porosity of sol–gel materials, which facilitates transport of gases or liquids through the material. Therefore, the structural properties are as important as their optical properties. The morphology of sol–gel based material is affected by the production process: solvent to precursor molar ratio, pH, catalyst, concentration of dopants, temperature, presence or absence of salts and additives, aging and drying conditions. Molar ratio R , pH and drying conditions are the most important variables that can affect the porous structure.

In this study, we examined the nanostructure of sol–gel films doped with photosensitizers in various concentrations. The surface roughness was measured by means of atomic force microscope in order to find out how the kind of photosensitizer and its concentration influence the surface smoothness of sol–gel films prepared with various molar ratios R .

2. Material preparation

The sol–gel materials under examination were produced from silica precursor tetraethoxysilan (TEOS $\text{Si}(\text{OC}_2\text{H}_5)_4$, 98%, Aldrich). The precursor was mixed with solvent (96% ethyl alcohol, Polish Chemicals) and catalyst (36% hydrochloric acid HCl, Polish Chemicals), to ensure acidic conditions ($\text{pH} \sim 2$). As a surfactant the Triton X-100 (from Aldrich) was used in the proportion of 20 μl per 2 ml of sol. The mixture was stirred up for 4 hours by means of magnetic stirrer at room temperature. A suitable amount of solvent was used so as to obtain the required molar ratio R , whereas R denotes the number of solvent moles (here ethanol) to the number of TEOS moles (see Table 1).

After the hydrolysis process, a homogeneous sol was obtained. The photosensitive agents photolon (from Haemato, Poland) and protoporphyrine PPIX (from Fluka) were used as dopants. The chemical structures of both photosensitizers are presented in Fig. 1.

Table 1. Proportion of substrates used for matrix preparation.

R factor	Ethanol C ₂ H ₅ OH [ml]	TEOS Si(OC ₂ H ₅) ₄ [ml]
20	26	5
32	43	5
40	52	5

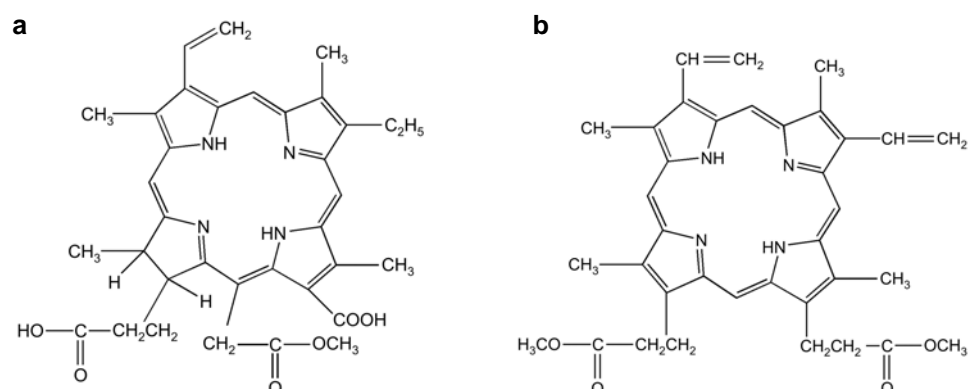


Fig. 1. Chemical structure of the photolon (a) and protoporphyrine (b) [7].

As one can see, both photosensitive agents have a similar structure. The size of a porphyrine molecule is about 0.7×0.7 nm (4 pyrrole units), so for PPIX it is 0.7×0.9 nm, thickness *ca.* 0.4 nm.

Three various sol–gel materials with molar ratios R equal to 20, 32, and 40 were produced. Two concentrations of photosensitizers were examined: *i.e.*, those of high concentration (of 0.5 mg/ml) and low concentration (of 0.05 mg/ml) sol was doped.

Samples were prepared in the form of films (single layer) deposited on microscopic slides (from Menzel-Glass, Germany). Microscopic slides were taken carefully from the box and immediately put in a beaker filled with 96% ethyl alcohol. The beaker was placed in ultrasonic bath for 30 min. Next, the slides were taken out and cleaned by a special cloth used for cleaning optical glasses. Next, 150 μ l of the photolon-doped sol or protoporphyrine IX-doped sol was dropped on the upper part of a slide placed at an angle of 45° and spread spontaneously onto its surface. Evaporation of the solvent led immediately to gel formation. Twelve different kinds of samples were prepared (see Tab. 2).

3. Measuring method

The nanostructure was examined by means of an AFM microscope, Quesant Instrument Corporation, California. The microscope worked in the contact mode, the tip had a height of 20 μ m, radius less than 10 nm, and cone angle less than 30° at the apex. A typical force constant of the cantilever is 0.15 Nm^{-1} and typical resonant

Table 2. Samples specification.

Sample	R ratio	Photosensitizer	Concentration
A	20	Protoporphyrine IX	High
B	32	Protoporphyrine IX	High
C	40	Protoporphyrine IX	High
D	20	Protoporphyrine IX	Low
E	32	Protoporphyrine IX	Low
F	40	Protoporphyrine IX	Low
G	20	Photolon	High
H	32	Photolon	High
I	40	Photolon	High
J	20	Photolon	Low
K	32	Photolon	Low
L	40	Photolon	Low

Table 3. Roughness amplitude parameters.

Symbol	Name	Unit
S_a	roughness average	[nm]
S_{sk}	surface skewness	—
S_y	peak–peak	[nm]

frequency is 12 kHz. The scan rate (the number of image lines scanned per second) was 1 Hz.

For each sample, 3 images of 800×800 nm were recorded. Next, the analysis was performed with the use of Scanning Probe Image Processor SPIP™. SPIP™ is a comprehensive product containing many analytical and visualization tools that can be applied to various types of images and curve data. It is also a precise tool for detailed surface characterization based on AFM images.

In this study, the surface roughness was measured. The roughness parameters as recommended in the European BCR Project “Scanning tunneling microscopy methods for roughness and micro hardness measurements” and additionally, some other parameters proposed by SPIP software, were calculated [12, 13].

Generally, the roughness parameters are divided into four groups: amplitude, hybrid, functional and spatial properties. For evaluation of the sol–gel matrices under examination 4 roughness parameters were chosen: roughness average, peak–peak height, surface skewness and fractal dimension.

3.1. Amplitude parameters

The amplitude properties of a sample are described by parameters which give information about the statistical average values, the shape of the height distribution histograms and about extreme properties (see Tab. 3).

The roughness average S_a gives information about the statistical average properties and is defined as:

$$S_a = \frac{1}{MN} \sum_{k=0}^{M-1} \sum_{l=0}^{N-1} |z(x_k, y_l) - \mu|$$

where M is the number of columns in the surface and N is the number of rows in the surface, with μ being the mean height:

$$\mu = \frac{1}{MN} \sum_{k=0}^{M-1} \sum_{l=0}^{N-1} z(x_k, y_l)$$

The average roughness is the most frequently used surface roughness parameter. It is the arithmetic mean or average of the absolute distances of the surface points from the mean plane.

The peak–peak height S_y is defined as the height difference between the highest and the lowest pixel in the image:

$$S_y = z_{\max} - z_{\min}$$

The surface skewness S_{sk} describes the asymmetry of the height distribution histogram. If $S_{sk} = 0$, a symmetric height distribution is indicated, for example, a Gaussian like. If $S_{sk} < 0$, it can be a bearing surface with holes and if $S_{sk} > 0$ it can be a flat surface with peaks. Values numerically greater than 1.0 may indicate extreme holes or peaks on the surface. The surface skewness is defined as:

$$S_{sk} = \frac{1}{MNS_a^3} \sum_{k=0}^{M-1} \sum_{l=0}^{N-1} [z(x_k, y_l) - \mu]^3$$

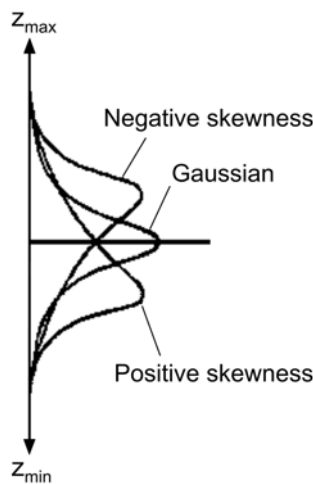


Fig. 2. Examples of the height distribution histogram [14].

were S_q is the root mean square:

$$S_q = \sqrt{\frac{1}{MN} \sum_{k=0}^{M-1} \sum_{l=0}^{N-1} [z(x_k, y_l) - \mu]^2}$$

Skewness measures the symmetry of the variation of a surface about its mean plane. A Gaussian surface, having a symmetrical shape for the height distribution, has a skewness of zero. A plateau honed surface with predominant plateau and deep valleys will tend to have a negative skew, whereas a surface comprised of disproportionate number of peaks will have positive skew (see Fig. 2).

3.2. Spatial parameters

Accurate information on amorphous or rather poorly crystallized structures, may be provided by fractal analysis. It is the instrument that can compute an important parameter: the fractal dimension S_{fd} .

The fractal dimension S_{fd} is calculated for the different angles by analyzing the Fourier amplitude spectrum. For different angles the Fourier profile is extracted and the logarithm of the frequency and amplitude coordinates is next calculated.

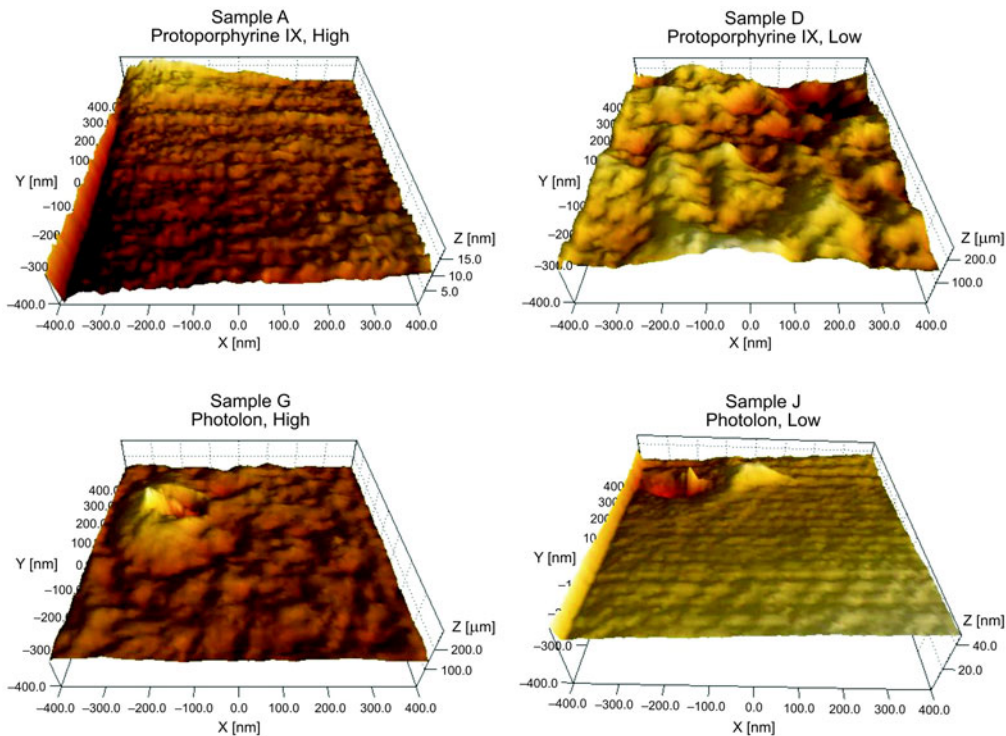


Fig. 3. AFM images of sol-gel films produced from sols with ratio $R = 20$, doped by photoagents in two various concentrations.

The fractal dimension for each direction is then calculated as 2.0 minus the slope of the log–log curves.

The fractal dimensions describing such fractal materials were found to be within the range $2 \leq S_{fd} < 3$: low S_{fd} values (2.0) indicate regularity and smoothness, intermediate S_{fd} values indicate irregular surfaces and S_{fd} values close to 3 indicate highly irregular surface.

4. Results

Analysis of AFM images revealed the fact that the sample texture depends on properties of substrates (ratio R), as well as photosensitizer concentrations. Exemples of AFM images are presented in Fig. 3.

The smallest roughness was observed for material doped with high concentration of protoporphyrine IX, independent of R factor. AFM images reflect very well the surface roughness (see also Fig. 4).

Figures 4–7 show the calculated roughness parameters of sol–gel materials, depending on R ratio, type of photosensitizer (Ph – photolon or PP – protoporphyrine) and its concentration (low or high).

Undoubtedly, photosensitizers used as dopants influence the smoothness of sol–gel matrix. This is confirmed by peak–peak height measurements (see Fig. 5),

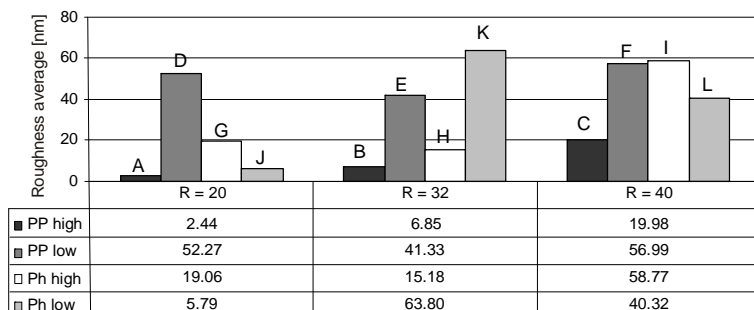


Fig. 4. Roughness average (Ph – photolon or PP – protoporphyrine).

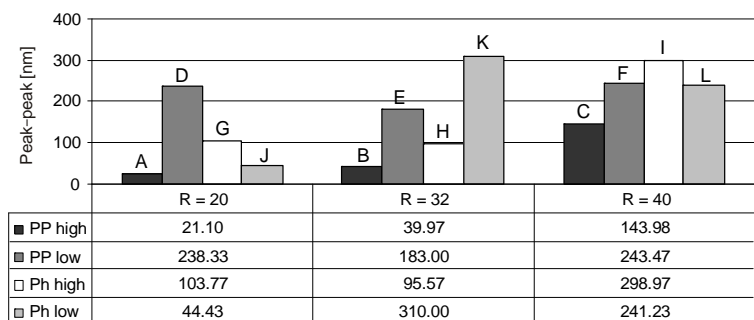


Fig. 5. Peak–peak height (Ph – photolon or PP – protoporphyrine).

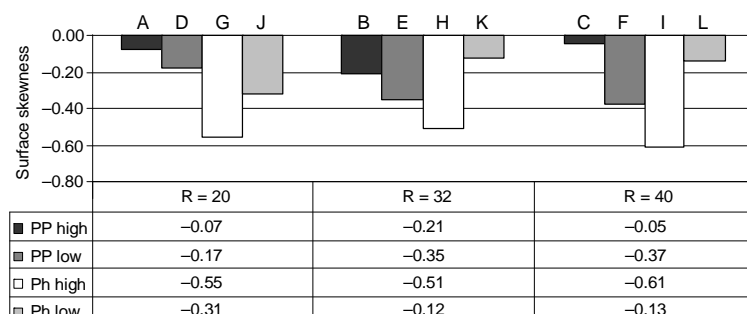


Fig. 6. Surface skewness (Ph – photolon or PP – protoporphyrine).

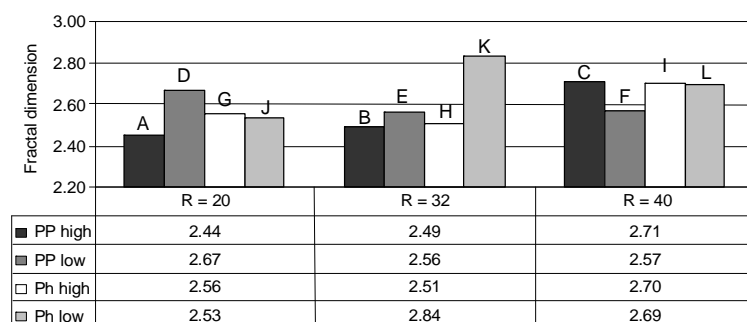


Fig. 7. Fractal dimension (Ph – photolon or PP – protoporphyrine).

where the lowest values are stated for material doped with high concentration of PPIX.

The surface skewness (Fig. 6) defines the asymmetry of the height distribution histogram. Firstly, we have got $S_{sk} < 0$, which means that the surface texture possesses holes and these are ordered in one direction (see Fig. 2). This phenomenon is a result of the way of material preparation (the sol flowed down on the slide inclined at an angle of 45°).

The fractal dimension values (see Fig. 7) in the range 2.20 to 2.90 indicate irregular surface texture. This result was observed especially for the material doped with photolon in low concentration with ratio $R = 32$ (sample K).

5. Discussion and conclusions

Analysis of the results obtained revealed the fact that porous sol–gel matrices show various characteristics, depending on the solvent content, which is, in our case, ethanol. Undoubtedly, R factor plays an important role in average roughness, peak–peak height and surface skewness. However, at this stage it is difficult to confirm the proportional dependences.

Comparing the samples we noticed that average roughness increases with increasing R factor for PPIX and photolon in higher concentration. This means that photosensitizers used as dopants influence the smoothness of sol–gel matrix. We also noticed that the smallest roughness is observed in the material doped with PPIX in higher concentration. This was stated for all the images analyzed. This indicates that sol–gel matrix enclosures the PPIX molecules resulting in smooth material.

Acknowledgments – The authors gratefully acknowledge financial support from the European Commission NANOTEC-EST Marie Curie ToK-Dev grant No 14059. We would also like to thank the Project Coordinator, Prof. Aurelia Meghea for her hospitality and scientific support.

References

- [1] VIJAYAKUMAR M., MURALIDHARAN P., VENKATESWARLU M., SATYANARAYANA N., *Sol–gel synthesis, structural characterization and ion transport studies of lithium samariumsilicate for lithium battery application*, Materials Chemistry and Physics **95**(1), 2006, pp. 16–23.
- [2] CHOI H., STATHATOS E., DIONYSIOU D.D., *Sol–gel preparation of mesoporous photocatalytic TiO₂ films and TiO₂/Al₂O₃ composite membranes for environmental applications*, Applied Catalysis B: Environmental **63**(1–2), 2006, pp. 60–7.
- [3] WENXIU QUE, UDDIN A., HU X., *Thin film TiO₂ electrodes derived by sol–gel process for photovoltaic applications*, Journal of Power Sources **159**(1), 2006, pp. 353–6.
- [4] MASAYUKI Y AMANE, *Unique commercial applications of the sol–gel process in Japan*, Journal of Sol–Gel Science and Technology **40**(2–3), 2006, pp. 273–9.
- [5] JERÓNIMO P.C.A., ARAÚJO A.N., MONTENEGRO M.C.B.S.M., *Optical sensors and biosensors based on sol–gel films*, Talanta **72**(1), 2007, pp. 13–27.
- [6] ALVARADO-MÉNDEZ E., ROJAS-LAGUNA R., ANDRADE-LUCIO J.A., HERNÁNDEZ-CRUZ D., LESSARD R.A., AVINA-CERVANTES J.G., *Design and characterization of pH sensor based on sol–gel silica layer on plastic optical fiber*, Sensors and Actuators B: Chemical **106**(2), 2005, pp. 518–22.
- [7] GOMES S.P., ODLOŽILÍKOVÁ M., ALMEIDA M.G., ARAÚJO A.N., COUTO C.M.C.M., MONTENEGRO M.C.B.S.M., *Application of lactate amperometric sol–gel biosensor to sequential injection determination of L-lactate*, Journal of Pharmaceutical and Biomedical Analysis **43**(4), 2007, pp. 1376–81.
- [8] DELMARRE D., MEALLET-RENAULT R., BIED-CHARRETON C., PASTERNAK R.F., *Incorporation of water-soluble porphyrins in sol–gel matrices and application to pH sensing*, Analytica Chimica Acta **401**(1–2), 1999, pp. 125–8.
- [9] DELMARRE D., BIED-CHARRETON C., *Grafting of cobalt porphyrins in sol–gel matrices: application to the detection of amines*, Sensors and Actuators B: Chemical **62**(2), 2000, pp. 136–42.
- [10] ULATOWSKA-JARZA A., PODBIELSKA H., BAUER J., MÜLLER G., BINDIG U., *Measurement of pectroscopic properties of sol–gel coated fiberoptic appliances*, Polish Journal of Environmental Studies **15**(4A), 2006, pp. 166–71.
- [11] PODBIELSKA H., ULATOWSKA-JARZA A., MÜLLER G. HOLOWACZ I., BAUER J., BINDIG U., *Silica sol–gel matrix doped with Photolon molecules for sensing and medical therapy purposes*, Biomolecular Engineering **27**(5), 2007, pp. 425–33, doi: 10.1016/j.bioeng.2007.07.005.
- [12] STOUT K.J., SULLIVAN P.J., DONG W.P., MAINSAH E., LUO N., MATHIA T., ZAHOUANI H., *The development of methods for the characterization of roughness on three dimensions*, Publication no. EUR 15178 EN of the Commission of the European Communities, Luxembourg 1994.

- [13] BARBATO G., CARNEIRO K., CUPPINI D., GARNAES J., GORI G., HUGHES G., JENSEN C.P., JORGENSEN J.F., JUSKO O., LIVI S., MCQUOID H., NIELSEN L., PICOTTO G.B., WILKENING G., *Scanning tunneling microscopy methods for roughness and micro hardness measurements*, Synthesis report for research contract with the European Union under its programme for applied metrology, European Commission Catalogue number: CD-NA-16145 EN-C, Brussels Luxembourg 1995.
- [14] Website of TrueGage Surface Metrology: <http://truegage.com/help/TrueMap/>.

*Received September 18, 2007
in revised form November 16, 2007*